Meteorological conditions, seasonal and annual mass balances of Chhota Shigri Glacier, western Himalaya, India

Mohd Farooq AZAM,[1,2,3] AL. RAMANATHAN,[2] P. WAGNON,[1,4] C. VINCENT,[5] A. LINDA,[2,6] E. BERTHIER,[7] P. SHARMA,[2] A. MANDAL,[2] T. ANGCHUK,[2] V.B. SINGH,[2] J.G. POTTAKKAL[2,8]

[1]*IRD/UJF – Grenoble I/CNRS/G-INP, LGGE UMR 5183, LTHE UMR 5564, 38402 Grenoble Cedex, France*
[2]*School of Environmental Sciences, Jawaharlal Nehru University, New Delhi, India*
[3]*Water Resources Systems Division, National Institute of Hydrology, Roorkee, India*
[4]*International Centre for Integrated Mountain Development, Kathmandu, Nepal*
[5]*UJF – Grenoble I/CNRS, LGGE UMR 5183, 38041 Grenoble Cedex, France*
[6]*Department of Environmental Sciences, School of Earth and Environmental Sciences, Central University of Himachal Pradesh, Dharamshala, India*
[7]*LEGOS, CNRS, Université de Toulouse, Toulouse, France*
[8]*Western Himalayan Regional Centre, National Institute of Hydrology, Jammu, India*
Correspondence: Mohd Farooq Azam <farooqaman@yahoo.co.in>

ABSTRACT. We present the updated glaciological mass balance (MB) of Chhota Shigri Glacier, the longest continuous annual MB record in the Hindu-Kush Karakoram Himalaya (HKH) region. Additionally, 4 years of seasonal MBs are presented and analyzed using the data acquired at an automatic weather station (AWS-M) installed in 2009 on a lateral moraine (4863 m a.s.l.). The glaciological MB series since 2002 is first recalculated using an updated glacier hypsometry and then validated against geodetic MB derived from satellite stereo-imagery between 2005 (SPOT5) and 2014 (Pléiades). Chhota Shigri Glacier lost mass between 2002 and 2014 with a cumulative glaciological MB of –6.72 m w.e. corresponding to a mean annual glacier-wide MB (B_a) of –0.56 m w.e. a^{-1}. Equilibrium-line altitude (ELA_0) for the steady-state condition is calculated as ~4950 m a.s.l., corresponding to an accumulation–area ratio (AAR_0) of ~61%. Analysis of seasonal MBs between 2009 and 2013 with air temperature from AWS-M and precipitation from the nearest meteorological station at Bhuntar (1050 m a.s.l.) suggests that the summer monsoon is the key season driving the interannual variability of B_a for this glacier. The intensity of summer snowfall events controls the B_a evolution via controlling summer glacier-wide MB (B_s).

KEYWORDS: accumulation, glacier mass balance, glacier meteorology, mountain glaciers

1. INTRODUCTION

The Hindu-Kush Karakoram Himalaya (HKH), covering a glacierized area of ~40 000 km^2 (Bolch and others, 2012), are the birthplace of some of the largest rivers in the world. The role of HKH glaciers as an important source of fresh water for the population living in the adjacent lowlands has been highlighted by several studies (e.g. Immerzeel and others, 2010; Kaser and others, 2010; Thayyen and Gergan, 2010), but these glaciers have not been monitored on a long-term basis (Bolch and others, 2012; Vincent and others, 2013). Mass-balance observations are needed to study the impact of climate change, especially in high remote areas such as the HKH region where meteorological observations are difficult and, thus, only recent and sparse (e.g. Fowler and Archer, 2006; Bhutiyani and others, 2010; Shekhar and others, 2010; Dimri and Dash, 2012). A contrasting pattern of glacier change has been observed throughout the HKH range, mainly revealed by studies using remote-sensing data (e.g. Fujita and Nuimura, 2011; Kääb and others, 2015).

The poor understanding of HKH glaciers has been highlighted in several recent studies (e.g. Cogley, 2009; Bolch and others, 2012; Vincent and others, 2013). Most of these studies attribute the major gaps in our knowledge of the behavior of these glaciers mainly to an insufficient number of in situ measurements, only partly substituted by remote-sensing studies (Bolch and others, 2012; Vincent and others, 2013). Obviously, ground-based observations are not possible for all glaciers in the HKH region, but they are necessary to validate/confirm the remotely sensed observations.

Chhota Shigri is a representative (Vincent and others, 2013) 'tier 2'-type (Paul and others, 2007) glacier in the Lahaul valley and has been studied for various aspects such as MB, ice thickness, surface velocity, MB reconstruction and energy balance (Wagnon and others, 2007; Azam and others, 2012, 2014a,b; Vincent and others, 2013). The goals of the present work are: (1) to understand the temporal and seasonal variability of meteorological parameters on Chhota Shigri Glacier using the glacier-side automatic weather station (AWS-M) data available between 2009 and 2013, (2) to discuss 12 years (2002–14) of annual glacier-wide MBs (B_a) and their validation against geodetic MB between 2005 and 2014, and (3) to present 4 years (2009–13) of measured seasonal (winter and summer) glacier-wide MBs (B_w and B_s) and analyze the meteorological control of B_a, B_w and B_s.

2. STUDY SITE AND AWS-M DESCRIPTION

Chhota Shigri Glacier (32.28° N, 77.58° E) is a valley-type, non-surging glacier located in the Chandra–Bhaga river basin

https://doi.org/10.3189/2016AoG71A570 Published online by Cambridge University Press

of Lahaul valley, Pir Panjal range, western Himalaya (Fig. 1). It extends from 5830 to 4050 m a.s.l. with a total length of 9 km and area of 15.48 km^2 in 2014 (Section 3). The ablation area comprises two main flows (Fig. 1), one coming from the eastern side of the accumulation area and the second from the western side. The lower ablation area (<4500 m a.s.l.) is covered by debris representing 3.4% of the total surface area (Vincent and others, 2013). Chhota Shigri Glacier is located in the monsoon–arid transition zone and is influenced by the Indian summer monsoon (ISM) during summer (July–September) and the Northern Hemisphere mid-latitude westerlies (MLW) during winter (January–April).

AWS-M is located off-glacier on a western lateral moraine (4863 m a.s.l.; Fig. 1) on a flat rocky surface and has been functioning continuously since 18 August 2009. The list of sensors installed on AWS-M, data gaps and treatments are provided in Azam and others (2014b). At the glacier base camp (3850 m a.s.l.; 2 km north of the glacier snout), an all-weather precipitation gauge with a hanging weighing transducer (Geonor T-200B) worked between 12 July 2012 and 10 October 2013 (Fig. 1).

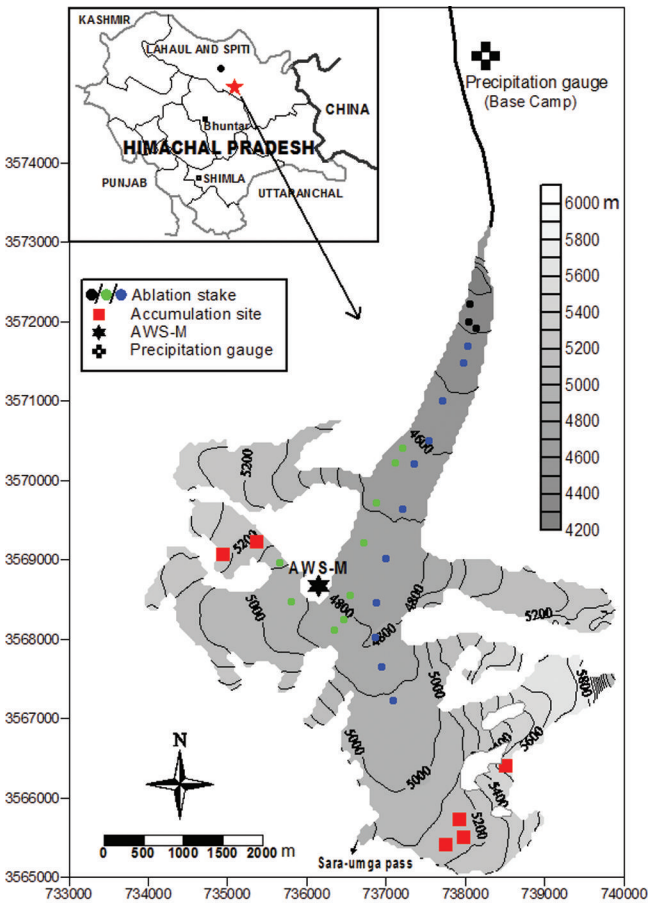

Fig. 1. Map of Chhota Shigri Glacier showing the ablation stakes on the debris-cover area (black dots), on the eastern flank (blue dots), on the western flank (green dots), accumulation sites (red squares), AWS-M (black star) and precipitation gauge (black cross). The map coordinates are in the UTM43 (north) World Geodetic System 1984 (WGS84) reference system.

3. FIELD MEASUREMENTS TO ASSESS THE MASS BALANCES

The hydrological year is defined from 1 October to 30 September of the following year on this glacier, mainly for practical reasons because access to the glacier is restricted after 15 October. The year is divided into summer (May–October) and winter (November–April) glaciological seasons. Annual glacier-wide surface MB measurements have been carried out on Chhota Shigri Glacier since 2002 at the end of September or beginning of October using the direct glaciological method (Paterson, 1994; Wagnon and others, 2007). The distribution of ablation and accumulation sites is shown in Figure 1. In October 2013, the electronic balance failed at an accumulation site, so the snow/firn core densities could not be calculated. We observed that from year to year, at a given location, the thickness of the annual snow/firn layer varies but the depth-averaged density remains almost the same. For instance, between 2009 and 2012, the mean depth-averaged density was 460 kg m^{-3} (standard deviation (STD) = 20 kg m^{-3}) at 5200 m a.s.l. on the western tributary and 480 kg m^{-3} (STD = 60 kg m^{-3}) at 5180 m a.s.l. on the eastern tributary. Therefore at each accumulation site, the mean vertical density in every pit for glaciological year 2012/13 was assumed equal to the mean depth-averaged density at this site from previous years.

Since 2002, the glaciological B_a of Chhota Shigri Glacier has been calculated using the glacier hypsometry (surface elevation distribution) obtained by combining two SPOT5 (Satellite Pour l'Observation de la Terre) digital elevation models (DEMs) (12 and 13 November 2004; 20 and 21 September 2005) (Wagnon and others, 2007). In every glaciological MB series, changing glacier area and elevation over time may give rise to some bias; therefore the glaciological MB series need to be recalculated (Zemp and others, 2013). The recent hypsometry of Chhota Shigri Glacier is calculated using a DEM derived from Pléiades images from 18 August 2014. In earlier publications, a small area of 0.10 km^2, located below the summit between 5830 and 6263 m a.s.l., has been systematically included in the MB calculations. However, visual examination of high-resolution Pléiades orthoimages suggested that this uppermost part is disconnected from the rest of the glacier. This small area is now excluded. The total glacierized area from Pléiades images in 2014, between 4050 and 5830 m a.s.l., is 15.48 km^2 while the glacierized area over the same altitudinal range from the 2005 SPOT5 images is 15.62 km^2. Thus between 2005 and 2014 the area decreased by 0.14 km^2 (0.9% of the 2005 area). Using these updated glacier outlines and hypsometries, we recalculated the B_a series assuming a linear area change (eqns 7 and 8 in Zemp and others, 2013) between 20–21 September 2005 and 18 August 2014, and considering 5830 m a.s.l. as the upper limit of the accumulation area. Chhota Shigri is a temperate glacier with thickness varying from 124 to 270 m in its ablation area (Azam and others, 2012). Such glaciers take a few decades (15–60 years) to adjust to their MB changes (Cuffey and Paterson, 2010), so one can expect a smooth change in area, especially over a short time period. The overall error in B_a, calculated following Thibert and others (2008), comes from a variance analysis applied to all types of errors (ice/snow density, core length, stake height determination, liquid-water content of the snow, snow height). Applying these errors at different altitudinal ranges, the uncertainty in B_a was calculated as ±0.40 m w.e. a^{-1}. The details of error estimation are provided in Azam and others (2012).

https://doi.org/10.3189/2016AoG71A570 Published online by Cambridge University Press

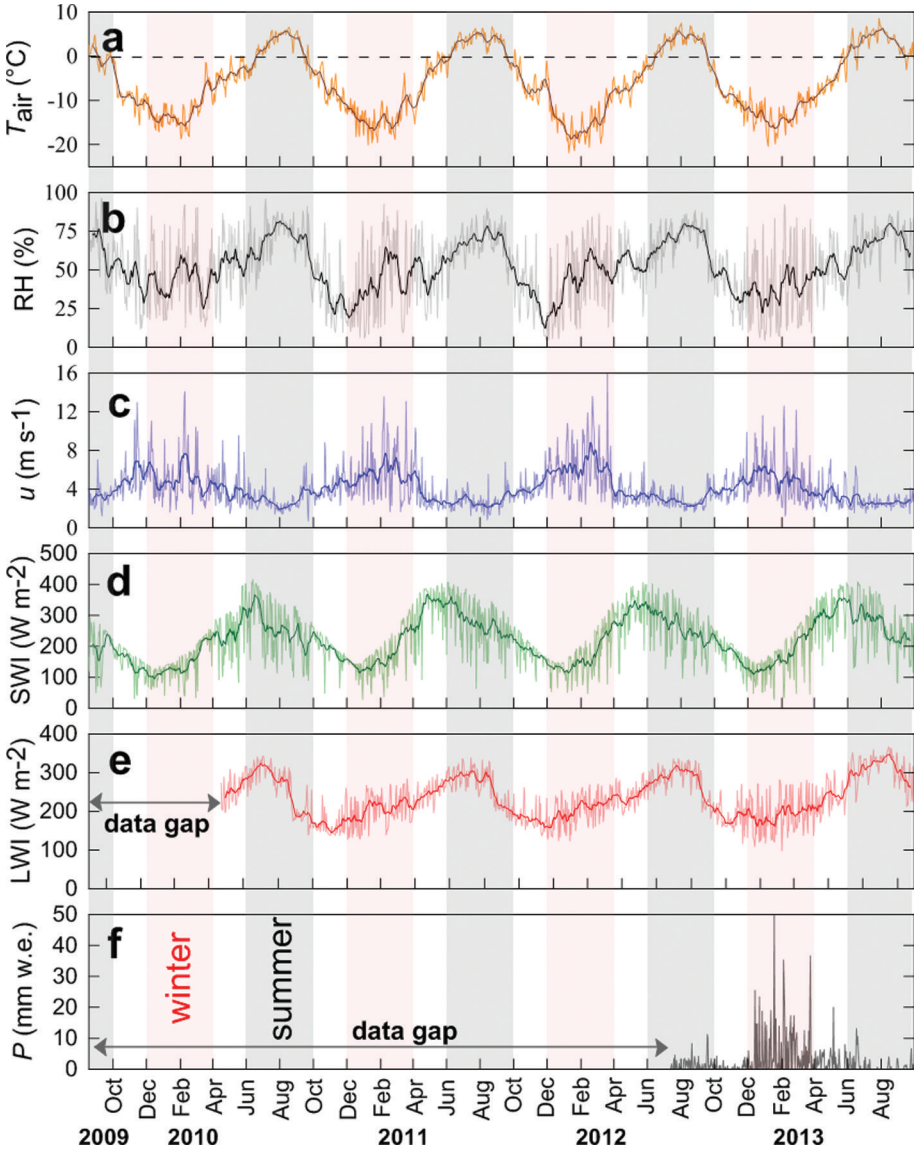

Fig. 2. Daily means of (a) air temperature T_{air} (°C), (b) relative humidity RH (%), (c) wind speed u (m s^{-1}), (d) incoming shortwave radiation SWI (W m^{-2}) and (e) incoming longwave radiation LWI (W m^{-2}) at AWS-M. T_{air}, RH, u and SWI are the daily means for the full observation period between 18 August 2009 and 30 September 2013, while LWI are the daily means between 23 May 2010 and 30 September 2013. (f) The daily precipitation (mm w.e.) between 12 July 2012 and 30 September 2013 collected by the precipitation gauge at glacier base camp. The thick lines in (a–e) are the 15 day running means.

4. RESULTS

4.1. Meteorological conditions on Chhota Shigri Glacier

Figure 2 displays the daily temporal variation in T_{air}, RH, u, SWI and LWI from 18 August 2009 to 30 September 2013 recorded by the AWS-M, and daily precipitation sums at glacier base camp recorded by the precipitation gauge between 12 July 2012 and 30 September 2013. Four hydrological years (1 October 2009 to 30 September 2013) for AWS-M variables and one hydrological year (1 October 2012 to 30 September 2013) for precipitation were selected to analyze the meteorological conditions at seasonal and annual scale. Based on local meteorology, Azam and others (2014b) delineated four seasons: summer monsoon (June–September), winter (December–March), pre-monsoon (April–May) and post-monsoon (October–November). For purposes of meteorological analysis, we adopt this subdivision of the annual cycle. Table 1 displays the mean annual and seasonal values of all studied variables for each hydrological year as well as for the whole period (1 October 2009 to 30 September 2013).

4.1.1. Air temperature and relative humidity

The monthly mean T_{air} during winter was –13.4°C and that for the summer monsoon was 2.5°C, while during pre-monsoon and post-monsoon it was –5.3°C and –7.8°C, respectively (Table 1). Whereas the monthly average T_{air} exceeds 0°C during at least three months (July–September), mean daily T_{air} can drop below the freezing point even in the hottest months of the year (21% of days in June, 5% in July, 3% in August and 15% in September). A sudden change in mean monthly T_{air} characterizes the onset of a new season; the most evident inter-seasonal change was found between the summer monsoon and post-monsoon, with a drop of 10.3°C, while the minimum difference (5.6°C) was found between post-monsoon and winter, showing that winter and the summer monsoon are thermally well distinguished. Compared to 2009/10, 2010/11 and

https://doi.org/10.3189/2016AoG71A570 Published online by Cambridge University Press

Table 1. Mean seasonal values of T_{air}, RH, u, SWI and LWI at AWS-M (4863 m a.s.l.). T_{air}, RH, u and SWI are the mean seasonal values of four hydrological years between 1 October 2009 and 30 September 2013 while LWI are the mean seasonal values between 1 June 2010 and 30 September 2013. P is the seasonal precipitation for one hydrological year between 1 October 2012 and 30 September 2013 at glacier base camp (3850 m a.s.l.) collected by the precipitation gauge

		Year				Mean
Season	Variable	2009/10	2010/11	2011/12	2012/13	
Post-monsoon (Oct–Nov)	T_{air} (°C)	–8.8	–7.3	–6.1	–9.1	–7.8
	RH (%)	48	35	33	40	39
	u (m s^{-1})	5.1	4.2	4.1	4.2	4.4
	SWI (W m^{-2})	150	191	186	178	176
	LWI (W m^{-2})	–	178	192	192	187
	P (mm w.e.)	–	–	–	32	–
Winter (Dec–Mar)	T_{air} (°C)	–12.4	–13.6	–14.5	–13.1	–13.4
	RH (%)	43	41	43	38	42
	u (m s^{-1})	5.1	5.5	6.3	5.0	5.5
	SWI (W m^{-2})	144	168	163	168	161
	LWI (W m^{-2})	–	190	195	190	192
	P (mm w.e.)	–	–	–	679	–
Pre-monsoon (Apr–May)	T_{air} (°C)	–4.6	–4.9	–6.1	–5.5	–5.3
	RH (%)	52	50	54	51	52
	u (m s^{-1})	3.9	3.4	3.4	3.5	3.5
	SWI (W m^{-2})	249	323	311	316	299
	LWI (W m^{-2})	–	230	233	231	231
	P (mm w.e.)	–	–	–	148	–
Summer monsoon (Jun–Sep)	T_{air} (°C)	1.9	2.8	2.4	3.3	2.5
	RH (%)	69	67	69	68	68
	u (m s^{-1})	2.9	2.7	2.9	2.7	2.8
	SWI (W m^{-2})	260	277	263	265	266
	LWI (W m^{-2})	280	276	283	308	289
	P (mm w.e.)	–	–	–	117	–
Annual (mean)	T_{air} (°C)	–5.7	–5.6	–6.1	–5.7	–5.8
	RH (%)	54	50	52	50	52
	u (m s^{-1})	4.1	4.0	4.3	3.8	4.1
	SWI (W m^{-2})	201	234	225	227	221
	LWI (W m^{-2})	–	224	230	237	230
	P (mm w.e.)	–	–	–	976	–

2011/12, the 2012/13 summer monsoon was relatively warm (0.8°C higher than the mean of the four hydrological years) while the 2009/10 winter season was warmer (1.0°C higher than the mean of the four hydrological years).

The highest peak in mean monthly relative humidity (RH) was observed in August (74%), while another peak was observed in February (51%) (Azam and others, 2014b). The summer monsoon mean RH was 68% and the winter season mean was 42%. Post-monsoon showed the lowest (39%) RH, while pre-monsoon showed the RH (52%) closest to the annual mean. The mean monthly RH between October and May was always lower than the annual mean (52%), while the lowest RH (33%) was observed in December. The 2011/12 summer monsoon showed the maximum RH (69%) whereas winter RH was minimum (38%) for 2012/13. Furthermore, a sudden drop in RH, noticed around 20 September (Fig. 2), shows the sharp decay of the monsoon on Chhota Shigri Glacier.

4.1.2. Precipitation

The automatic precipitation gauge (3850 m a.s.l.; Fig. 1) provides the only recorded local precipitation data for Chhota Shigri Glacier. Table 1 shows the seasonal precipitation sums for a single complete hydrological year between 1 October 2012 and 30 September 2013. The observed precipitation during winter was maximum, with a contribution of 71% to the total annual precipitation, whereas post-monsoon received minimum precipitation (3% of the annual amount). The contributions of pre-monsoon and summer monsoon to annual precipitation were only 15% and 12%, respectively. Although 71% of the precipitation occurred during the 2012/13 winter season, the mean winter season RH was low (38%) (Table 1). This is because the MLW bring moisture in the form of strong storms (Lang and Barros, 2004) which are generally short, with a life span of 2–4 days, but provide important amounts of precipitation (Dimri and Mohanty 2009). This interpretation is supported by Figure 2b, where RH occasionally peaked to very high values during winter, but otherwise this season is mostly very dry. By contrast, the monsoon is a constantly humid season (high RH), with frequent but light precipitation resulting in total amounts of precipitation that are lower than in winter. Therefore, unlike the summer-accumulation type glaciers (Ageta and Higuchi, 1984) in the central Himalaya, Chhota Shigri Glacier seems to receive most of its precipitation in winter. The monthly precipitation sums (not shown in Table 1) were highest in January and February (183 and 238 mm, respectively), whereas the lowest were in October and November (14 and 18 mm, respectively). The precipitation minimum during October and November, in agreement with studies in the neighboring Beas Basin (e.g. Prasad and Roy, 2005; Datt and others, 2008), supports the choice of the hydrological year starting from 1 October. However, these analyses should be

https://doi.org/10.3189/2016AoG71A570 Published online by Cambridge University Press

regarded with caution as they are based on a single year of precipitation. A long-term precipitation record from glacier base camp is desirable to definitely state whether or not Chhota Shigri is a winter-accumulation type glacier.

4.1.3. Incoming short- and longwave radiations

SWI was highest during the pre-monsoon. As soon as the summer monsoon starts, T_{air} increases but SWI is reduced in agreement with high RH (Fig. 2; Table 1) (Azam and others, 2014b). The LWI was highest during the summer monsoon because of high emission from the summer-monsoonal clouds. The post-monsoon and winter season exhibited similar conditions. The mean monthly LWI was highest (336 W m^{-2}) in August 2013 and lowest (165 W m^{-2}) in December 2010, whereas the mean monthly SWI was highest (344 W m^{-2}) in May 2011 and lowest (107 W m^{-2}) in December 2009.

4.1.4. Wind regimes

On average, u was highest during the winter season, with a mean value of 5.5 m s^{-1}, reaching its maximum monthly value of 6.2 m s^{-1} in February. u was also strong in pre-monsoon (mean 3.5 m s^{-1}), especially in March (monthly mean 5.1 m s^{-1}). u over the summer monsoon was quite weak (mean 2.8 m s^{-1}) with a minimum speed in August (monthly mean 2.4 m s^{-1}). During the post-monsoon, wind speeds were moderate (mean 4.4 m s^{-1}) and approached the high speed of wintertime. The summer monsoon winds were almost the same for the four hydrological years, while the winter wind exhibited more interannual variability, with the highest speed measured during the 2011/12 hydrological year. A decrease in u during the first half of May (Fig. 2) can be considered as the onset of the monsoon on Chhota Shigri Glacier. Indeed, Shea and others (2015), based on records from five high-altitude meteorological stations in the Nepalese Himalaya, showed that the monsoon, as soon as it starts, is characterized by relatively calm conditions (daily wind speeds are generally <4 m s^{-1}).

4.2. Annual and seasonal mass balances

4.2.1. Spatial pattern of point mass balances

Figure 3a–h show the point MBs as a function of altitude for hydrological years 2006–14 (for 2002–06, see Wagnon and others, 2007). Ablation at the stakes (black dots) in the lowest part of the ablation area is subdued by 2–3 m w.e. a^{-1} irrespective of their altitude (Fig. 3a–h). This is due to the debris cover, which has an insulating effect, and the deep, narrow valley which reduces incoming shortwave radiation (Wagnon and others, 2007). However, the annual point MBs are still very negative on the debris-covered area, with annual values varying between –2 and –5 m w.e.

Given the harsh conditions and rugged terrain, the point accumulation measurements at 5500/5550 m a.s.l. could only be carried out in 2003, 2004, 2005, 2009 and 2011. For the years without accumulation measurements at 5500/5550 m a.s.l., an extrapolation of 5200 m a.s.l. mean MB (three measurements in the eastern part) to 5500/5550 m a.s.l. was done applying the MB gradient calculated between 5200 and 5500/5550 m a.s.l. from point-MB profiles in similar years (the years with almost the same point annual MBs up to 5200 m a.s.l.). Accumulation at 5500/5550 m a.s.l. on the eastern flank (main glacier) varied between a minimum annual value of 1.0 m w.e. in 2006/07 (extrapolated) and a maximum value of 2.3 m w.e. in the 2008/09 (measured) hydrological year.

4.2.2. Annual vertical mass-balance gradients

The blue lines in Figure 3a–h are the regression lines fitted to annual point MBs measured on the debris-free part of the main glacier body (eastern flank) between 4400 and 5200 m a.s.l. These regression lines were used to derive the vertical MB gradients (db/dz) for each hydrological year. The annual db/dz are reported in Table 2. Over the 2002–14 observation period, the annual db/dz between 4400 and 5200 m a.s.l. showed a STD of 0.09 m w.e. (100 m)$^{-1}$ with a minimum value of 0.52 m w.e. (100 m)$^{-1}$ for 2008/09 and a maximum value of 0.81 m w.e. (100 m)$^{-1}$ for 2011/12. The mean db/dz between 2002 and 2014 was 0.66 m w.e. (100 m)$^{-1}$, which is in good agreement with the mean db/dz of 0.69 m w.e. (100 m)$^{-1}$ calculated over a small altitudinal range (4400–4900 m a.s.l.) between 2002 and 2006 on Chhota Shigri Glacier (Wagnon and others, 2007).

The annual db/dz over the debris-covered part of the glacier is negative, due to a decrease in the debris thickness (and in turn of its resulting insulating effect) as a function of altitude. However, given the short altitudinal range (only 100 m between stakes installed at 4300 and 4400 m a.s.l.), any quantification of this db/dz would be speculative and not statistically significant. The annual db/dz in the accumulation area (Fig. 3) showed rather less annual variability (STD = 0.08 m w.e. (100 m)$^{-1}$), with a low mean value of 0.22 m w.e. (100 m)$^{-1}$ between 2002 and 2014. The mean accumulation db/dz was calculated using field-observed accumulation db/dz available for only five years (Table 2).

4.2.3. Annual and cumulative glacier-wide mass balances

The recalculated B_a of Chhota Shigri Glacier between 2002 and 2014 are given in Table 2, whereas Figure 4 displays the B_a as well as the cumulative glacier-wide MB over the same period. The recalculation changed the B_a up to 0.05 m w.e. a^{-1}. B_a was generally negative, except for four years (2004/05, 2008/09, 2009/10 and 2010/11) when it was slightly positive. B_a varied from a minimum value of -1.43 ± 0.40 m w.e. in 2002/03 to a maximum value of $+0.32 \pm 0.40$ m w.e. in 2009/10 and had a large interannual variability (STD = 0.65 m w.e. a^{-1}). The cumulative glacier-wide MB of Chhota Shigri was –6.72 m w.e. between 2002 and 2014, corresponding to a B_a of -0.56 ± 0.40 m w.e. a^{-1}.

4.2.4. ELA and AAR

Table 2 shows the equilibrium-line altitude (ELA) and accumulation–area ratio (AAR) for each hydrological year between 2002 and 2014. ELA was calculated using the regression line (blue lines in Fig. 3) extracted through the annual point MBs of the main glacier body (eastern flank) between 4400 and 5200 m a.s.l. The AAR for each year is then calculated using the ELA of the corresponding year. Since 2002 the ELA has varied from a maximum value of 5235 m a.s.l. in 2002/03 ($B_a = -1.43 \pm 0.40$ m w.e.; AAR = 24%) to a minimum value of 4905 m a.s.l. in 2004/05 ($B_a = +0.13 \pm 0.40$ m w.e. and AAR = 69%). The annual ELA and AAR showed a good correlation with B_a ($r^2 = 0.94$ and 0.94, respectively) between 2002 and 2014 (Fig. 5). The ELA for a zero B_a (ELA$_0$) was also derived from the regression between B_a and ELA over 2002–14, and calculated as

https://doi.org/10.3189/2016AoG71A570 Published online by Cambridge University Press

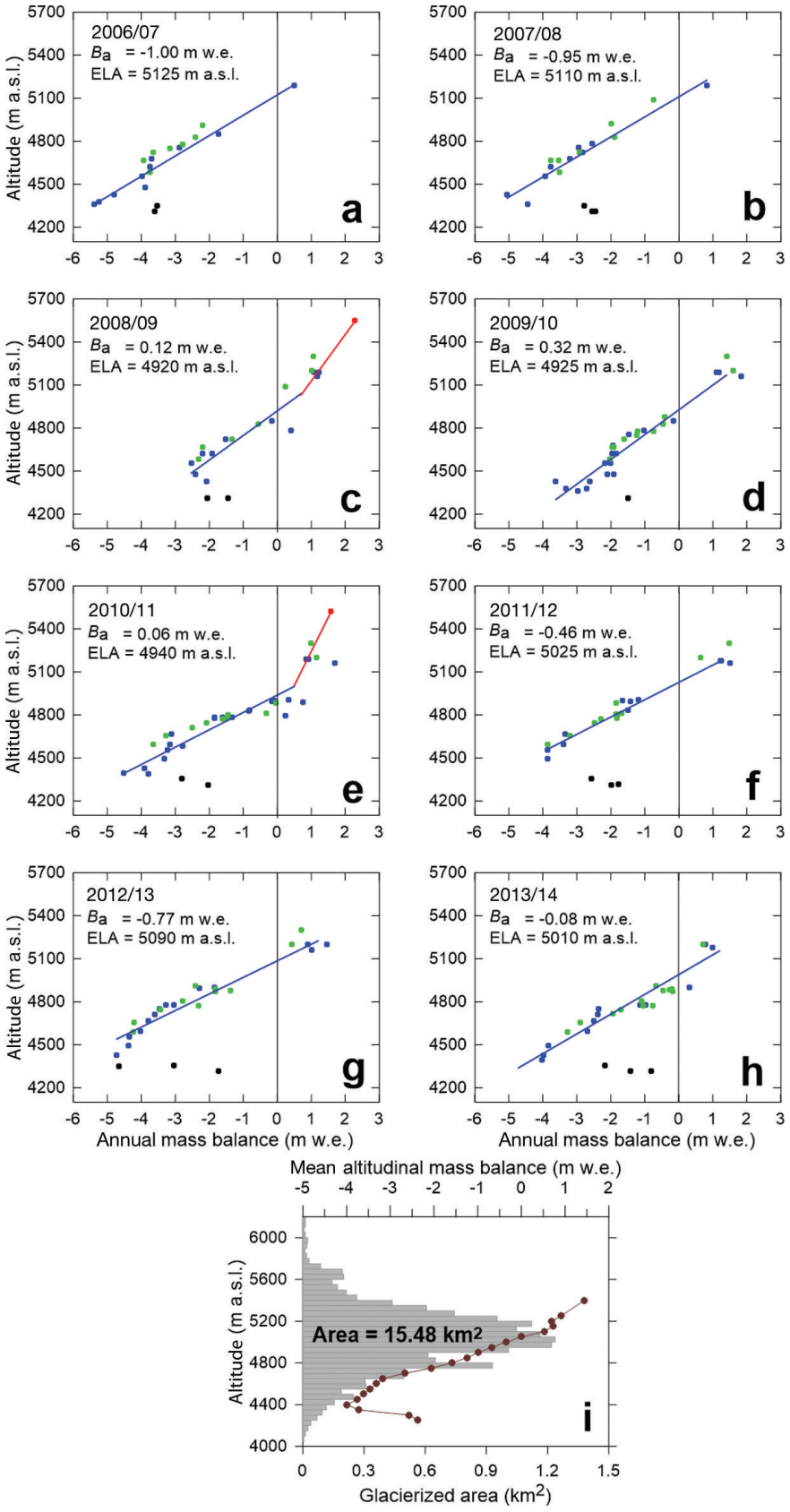

Fig. 3. (a–h) The annual point MB (dots) as a function of altitude derived from field measurements (stakes, drillings or pits) on Chhota Shigri Glacier for eight hydrological years between 2006 and 2014. Measurements were performed on 30 September 2006, 1 October 2007, 6 October 2008, 9 October 2009, 10 October 2010, 9 October 2011, 10 October 2012, 6 October 2013 and 4 October 2014 (±4 days). The black, blue and green dots are the annual point MBs over the debris-cover area (<4400 m a.s.l.), the eastern flank and the western flank of the glacier, respectively, whereas red dots are the MBs at 5500/5550 m a.s.l. The blue and red lines are the regression lines fitted to point annual MBs in the ablation and accumulation parts of the eastern flank, respectively. B_a and ELA for each year are also displayed on the corresponding panel. (i) The hypsometry (50 m altitudinal ranges) and mean (2002–14) altitudinal MBs (brown dots) of Chhota Shigri Glacier. The mean altitudinal MBs are mean MBs for each 50 m range (e.g. 4400 MB represents the mean MB for 4400–4450 range), except at 4250 and 5400 where the mean MBs are for 4050–4300 and 5400–5830 range, respectively.

https://doi.org/10.3189/2016AoG71A570 Published online by Cambridge University Press

Table 2. Annual and seasonal MBs, ELA, AAR and MB gradients db/dz (m w.e. (100 m)$^{-1}$) for Chhota Shigri Glacier. The subscripts abl and acc stand for ablation zone (4400–5200 m a.s.l.) and accumulation zone (5200–5830 m a.s.l.), respectively. The mean and STD are also displayed for every variable. The uncertainty range for B_a is ±0.40 m w.e. (Azam and others, 2012)

	2002/03	2003/04	2004/05	2005/06	2006/07	2007/08	2008/09	2009/10	2010/11	2011/12	2012/13	2013/14	**mean**	**STD**
B_a (m w.e.)	–1.43	–1.24	0.13	–1.43	–1.00	–0.95	0.12	0.32	0.06	–0.46	–0.77	–0.08	**–0.56**	**0.65**
ELA (m a.s.l.)	5235	5105	4905	5230	5125	5110	4920	4925	4940	5025	5090	5010	**5052**	**116**
AAR (%)	24	39	69	22	37	39	67	64	66	52	36	54	**47**	**17**
db/dz_{abl} (m w.e. (100 m)$^{-1}$)	0.62	0.74	0.62	0.61	0.68	0.68	0.52	0.54	0.73	0.81	0.76	0.64	**0.66**	**0.09**
db/dz_{acc} (m w.e. (100 m)$^{-1}$)	0.29	0.18	0.25	–	–	–	0.3	–	0.1	–	–	–	**0.22**	**0.08**
B_w (m w.e.)	–	–	–	–	–	–	–	1.19	0.97	1.18	0.76	–	**1.02**	**0.20**
B_s (m w.e.)	–	–	–	–	–	–	–	–0.87	–0.91	–1.64	–1.53	–	**–1.24**	**0.40**
*Meteorological conditions**														
Annual temperature (°C)	–	–	–	–	–	–	–	–5.7	–5.6	–6.2	–5.8	–	**–5.8**	**0.3**
Summer temperature (°C)	–	–	–	–	–	–	–	1.3	2.7	2.5	3.2	–	**2.4**	**0.8**
Winter temperature (°C)	–	–	–	–	–	–	–	–10.1	–9.0	–9.9	–8.5	–	**–9.4**	**0.8**
Annual precipitation (mm)	–	–	–	–	–	–	–	1187	1130	825	939	–	**1020**	**168**
Summer precipitation (mm)	–	–	–	–	–	–	–	766	493	402	228	–	**472**	**225**
Winter precipitation (mm)	–	–	–	–	–	–	–	421	637	423	711	–	**548**	**149**

*Temperature at AWS-M (4863 m a.s.l.) and precipitation at Bhuntar meteorological station (1092 m a.s.l.). For the summer or winter means, the starting and ending dates have been chosen to match the field measurements of B_s and B_w, respectively.

~4950 m a.s.l. Similarly AAR_0 was calculated as ~61% for steady-state B_a (Fig. 5).

4.2.5. Seasonal glacier-wide mass balances

On Chhota Shigri Glacier, seasonal MB measurements were started in May 2010 to assess the winter (B_w) and summer glacier-wide MBs (B_s) separately. Access to the glacier at the end of winter depends on road clearance, so B_w observations could not be carried out on fixed dates. The measurements were performed on 21 May 2010, 24 June 2011, 20 June 2012 and 6 July 2013 (±3 days). Azam and others (2014a) suggested that the average summer ablation period lasts 96 ± 18 days from mid-June to the end of September and neither ablation nor accumulation is dominant during May–June. Therefore, no correction was applied to the field B_w for varying measurement dates. Table 2 and Figure 6 show the seasonal MBs. B_w ranged from a maximum value of 1.19 m w.e. in 2009/10 to a minimum value of 0.76 m w.e. in 2012/13, whereas B_s varied from –0.87 m w.e. in 2009/10 to –1.64 m w.e. in 2011/12. Between 2009 and 2013, the observed B_a on Chhota Shigri Glacier was slightly positive for 2009/10 (0.32 m w.e.) and 2010/11 (0.06 m w.e.) and negative for 2011/12 (–0.46 m w.e.) and 2012/13 (–0.77 m w.e.). The separation of seasonal MBs over this period is crucial to understand the causes for positive and negative balance years (Section 5.2).

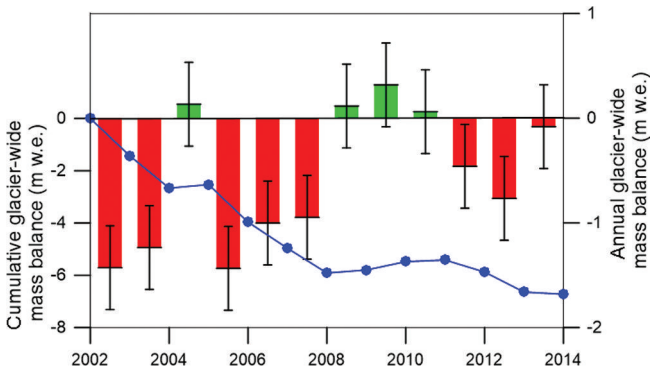

Fig. 4. Cumulative (blue dots) and annual glacier-wide mass balances (red (–) and green (+) histograms) of Chhota Shigri Glacier between 2002 and 2014. Error bars represent the uncertainty in annual glacier-wide mass balance calculated in Azam and others (2012).

4.2.6. Geodetic glacier-wide mass balance

The 2005–14 glacier-wide geodetic MB has been computed using DEMs derived from SPOT5 and Pléiades stereo-images. The 2005 SPOT5 DEM was derived from a stereo-pair acquired on 20 and 21 September 2005 by the SPOT5-HRG sensor with a resolution of 2.5 m. The 2014 DEM was derived from Pléiades stereo-images acquired on 18 August 2014. The methodology followed to compute the Pléiades DEM, to adjust horizontally and vertically the two DEMs on the ice-free terrain and to estimate the glacier-wide MB has been described in detail for similar datasets acquired over the Mont Blanc area, European Alps (Berthier and others, 2014). Given the similarity of the imagery used over Chhota Shigri Glacier to that used in the Mont Blanc study, we also used the uncertainties estimated over Mont Blanc glaciers using GPS measurements. Elevation changes from SPOT5/Pléiades DEM differencing were found to be accurate within ±1.3 m and this error level was conservatively multiplied by a factor of 5 for regions where at least one of the DEMs had data gaps. In the case of Chhota Shigri Glacier, these unsurveyed areas cover ~23% of the total

https://doi.org/10.3189/2016AoG71A570 Published online by Cambridge University Press

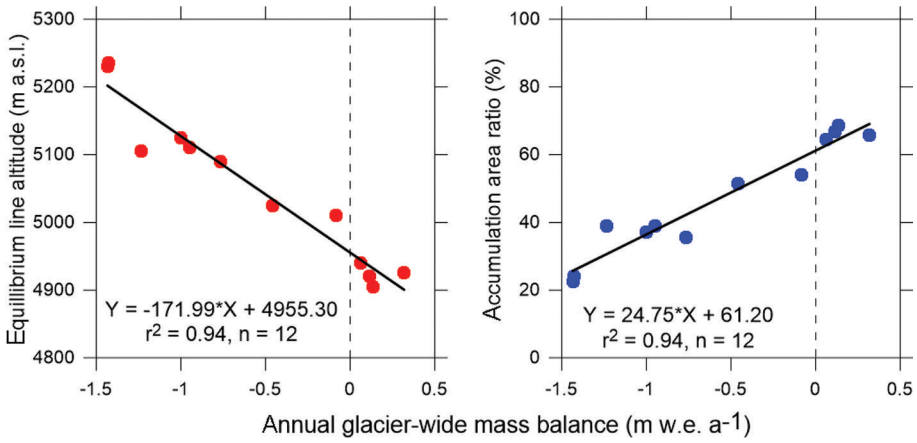

Fig. 5. The ELA and AAR as a function of annual glacier-wide mass balance.

glacier area. Between 21 September 2005 and 18 August 2014, the total elevation change is -3.55 ± 2.52 m, corresponding to a mean annual rate of -0.40 ± 0.28 m a^{-1}. We converted this elevation change to a glacier-wide MB of -3.02 ± 2.15 m w.e. using a density of 850 ± 60 kg m^{-3} (Huss, 2013).

5. DISCUSSION

5.1. Annual mass balances

This unique MB dataset in the HKH region shows that Chhota Shigri Glacier, previously found to be representative of the whole Lahaul and Spiti region (2110 km^2; Vincent and others, 2013), has been losing mass since 2002 at a mean rate of –0.56 m w.e. a^{-1}. Even though the Chhota Shigri MB series is the longest in the HKH region, 12 years of measurements is still too short to extract any statistically significant trend of MB, highlighting the need for this valuable series to be maintained over the long term so that the glacier may be used as a climatic indicator. Moreover, this dataset provides reliable data on ELA–B_a or AAR–B_a relationships that could be used to reconstruct the MB series in time or to spatially extrapolate it. Recently, Brun and others (2015) used Moderate Resolution Imaging Spectroradiometer (MODIS) images of Chhota Shigri Glacier, and reconstructed the MB series between 1999 and 2013. They obtained MB of –0.82, –1.09 and –0.94 m w.e. a^{-1} for 1999/2000, 2000/01 and 2001/02, respectively. Combining these data with our glaciological series, the cumulative MB is then calculated as –8.27 m w.e. between 1999 and 2011, corresponding to -0.69 ± 0.40 m w.e. a^{-1}, which is in reasonable agreement with the value reported by Gardelle and others (2013) who calculated a region-wide MB of -0.45 ± 0.13 m w.e. a^{-1} for the 2110 km^2 area in Lahaul and Spiti, western Himalaya, between 1999 and 2011. Kääb and others (2012) calculated an elevation change of -0.77 ± 0.08 m a^{-1} for a 2° latitude × 2° longitude cell around Chhota Shigri Glacier between 2003 and 2008. This elevation change is converted, using an ice density of 900 kg m^{-3}, to a mass loss of -0.69 ± 0.07 m w.e. a^{-1}. Over the same period, the mean B_a of Chhota Shigri Glacier is also in agreement with a value of -0.90 ± 0.40 m w.e. a^{-1}.

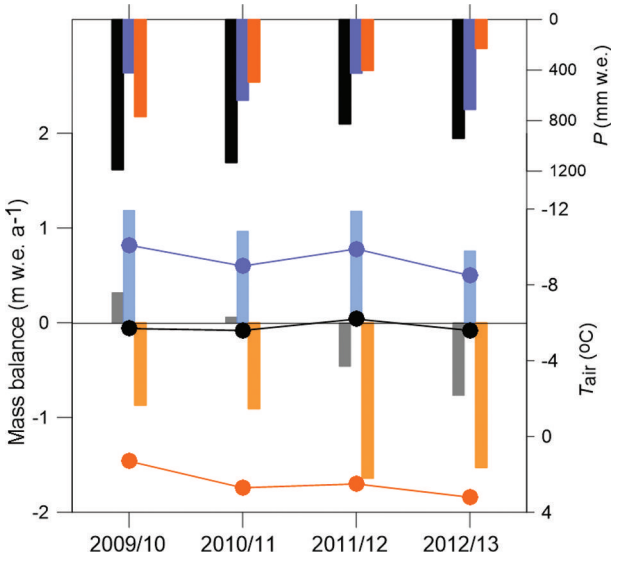

Fig. 6. Annual, winter and summer mass balances are shown by, respectively, gray, light blue and light orange histograms. The annual, winter, summer precipitations and temperatures are shown by black, blue, orange histograms and dots respectively. The mean temperatures are from AWS-M while the precipitation sums are from Bhuntar meteorological station.

The MB gradients (Table 2) calculated over the debris-free ablation area of Chhota Shigri Glacier are comparable to those observed in the European Alps, Nepalese Himalaya and other mid-latitude regions (e.g. Rabatel and others, 2005; Zemp and others, 2009; Shea and others, 2013; Wagnon and others, 2013). Some recent studies (e.g. Racoviteanu and others, 2013) developed glacier melt models at watershed scale in the Himalayan region based on a single ablation gradient. Such models can therefore be improved in the future using different MB gradients for different glacier zones (debris-covered, ablation and accumulation areas).

5.2. Seasonal mass balances

Azam and others (2014b), using a surface energy-balance (SEB) approach, analyzed the impact of the ISM on Chhota Shigri Glacier B_a and concluded that the intensity of snowfall events during the summer monsoon is among the most important drivers controlling B_a via enhancing summer accumulation and limiting ablation. The snowfalls during the summer monsoon cover the glacier surface and control the glacier albedo and thus the amount of absorbed

https://doi.org/10.3189/2016AoG71A570 Published online by Cambridge University Press

shortwave radiation, which is the main heat source for the Himalayan glaciers (Azam and others, 2014b).

Although the seasonal MBs are available only between 2009 and 2013, this series still provides a first preliminary opportunity to analyze how the seasonal MBs determine B_a. In order to understand the influence of the meteorological conditions on seasonal MBs and in turn on B_a, the annual and seasonal MBs were compared with the meteorological data (Table 2; Fig. 6). In situ temperature (T_{air}) records from the AWS-M (4863 m a.s.l.) were used for this analysis, while precipitation (P) data were taken from the precipitation record at Bhuntar meteorological station (1092 m a.s.l.; ~50 km southwest of Chhota Shigri Glacier; Fig. 1). For a proper comparison, B_a, B_w and B_s were compared with annual, winter and summer T_{air} and P over identical periods, matching the dates of MB field measurements.

The relationship between B_a and annual P was consistent, with a positive deviation from the mean during positive B_a years (precipitation anomaly of +167 and +110 mm in 2009/10 and 2010/11, respectively, compared to the 2009–13 mean of 1020 mm) and a negative deviation during negative years (precipitation anomaly of –195 and –81 mm, in 2011/12 and 2012/13, respectively). At seasonal scale, we could not find any relationship between B_w and winter P. Contrary to B_w, B_s showed a good agreement with summer P: in 2009/10 and 2010/11, the B_s were less negative (–0.87 and –0.91 m w.e., respectively) with higher summer P (precipitation anomaly of +294 and +21 mm, respectively, compared to the 2009–13 mean of 472 mm) whereas in 2011/12 and 2012/13 the B_s were more negative (–1.64 and –1.53 m w.e., respectively) with lower summer P (precipitation anomaly of –70 and –244 mm, respectively, compared to the 2009–13 mean).

The annual mean deviations from the mean annual T_{air} (–5.8°C) were small: +0.1, +0.2, –0.4 and 0.0°C in 2009/10, 2010/11, 2011/12 and 2012/13, respectively, which prevents any reliable examination of the relation between B_a and annual T_{air}. Nevertheless B_w values were consistent with winter T_{air} (Fig. 6), with a negative deviation (temperature anomaly of –0.7°C and –0.5°C, respectively) from the mean (–9.4°C) during the high B_w years (2009/10 and 2011/12) and a positive deviation (temperature anomaly of +0.4°C and +0.9°C, respectively) during the low B_w years (2010/11 and 2012/13). B_s also showed a consistent relationship with summer mean T_{air}, except for 2010/11 when summer T_{air} was slightly higher (+0.3°C) than the mean summer T_{air} (2.4°C) between 2009 and 2013 but B_s was less negative (–0.91 m w.e.).

Even though the mean summer monsoon T_{air} at AWS-M was positive during the 4 years (Table 1), daily mean T_{air} occasionally dropped below the freezing point (Section 4.1.1; Fig. 2) during summer months, indicating that precipitation may sometimes occur as snow. This was probably the dominant case in 2009/10 and 2010/11 positive B_a years (with positive precipitation anomaly) compared to the other years. These snowfalls changed the surface albedo of the glacier during the high melting period of summer, so the melting was reduced, leading to less negative B_s for 2009/10 and 2010/11. Given that in 2011/12 and 2012/13 negative B_a years, summer T_{air} were slightly higher and P were lower than their mean values between 2009 and 2013, the snowfalls were probably sporadic and not heavy enough to protect the glacier from higher melting. These years were thus characterized by highly negative B_s.

The present analysis at seasonal scale is in agreement with the findings of our earlier detailed SEB study (Azam and others, 2014b). This key impact of wet-season snowfalls via the albedo effect during the melt season has already been described in other parts of High Mountain Asia (e.g. Fujita, 2008; Zhang and others, 2013) and elsewhere (e.g. Sicart and others, 2011). In the central Tibetan Plateau, Mölg and others (2012) analyzed the impact of ISM on Zhadang Glacier using a fully distributed SEB/MB model between 2009 and 2011 and concluded that the timing of monsoon onset leaves a clear footprint on the glacier via the albedo effect.

Although Chhota Shigri Glacier receives maximum precipitation during winter (Section 4.1.2), the present analysis suggests that summer is the key season for this glacier. During summer months the ablation and accumulation coincide and the intensity of summer accumulation controls the B_a evolution through B_s. However, we believe that the unclear link between B_w and winter P needs to be clarified and this analysis should be developed with long-term comparison of seasonal MBs with meteorological variables to reach more robust conclusions.

5.3. Validation of glaciological mass-balance series

It is recommended that the glaciological MB series be validated with geodetic MB to detect the potential systematic biases in glaciological MB series (e.g. Zemp and others, 2013). Given the harsh high-altitude conditions of the HKH region, access to the accumulation area is often difficult, which limits the number of point accumulation measurements; therefore, it becomes even more essential to check the glaciological MB series. In the HKH region, the glaciological MB series are generally very short and never validated using geodetic MB.

To be meaningful, the comparison must be done over matching periods. The glaciological MBs have generally been calculated from the first week of October to the first week of October of the following year between 2002 and 2014, whereas the geodetic MB was calculated between 21 September 2005 and 18 August 2014. Therefore an adjustment is necessary to calculate the geodetic MB for nine full years (between 21 September 2005 and 21 September 2014). The MB reconstruction model (Azam and others, 2014a) is used to make this adjustment to geodetic MB. Unfortunately the meteorological data (between 18 August and 21 September 2014) needed to run the model were not available at the time of writing. Thus the mean reconstructed MB between 18 August and 21 September during 1969–2013 (–0.52 m w.e. with a STD of 0.20 m w.e.) is added to the geodetic MB (–3.02 ± 2.15 m w.e. from 21 September 2005 to 18 August 2014) to extend it over the full 9 year period until 21 September 2014, leading to a cumulative mass balance of –3.54 m w.e., equivalent to –0.39 m w.e. a^{-1}. Nevertheless, there is still a shift of ~10 days in both methods, as glaciological MB is calculated from the first week of October to the first week of October of the following year, but this is acceptable as the shift is systematic. The cumulative glaciological MB between 2005 and 2014 is calculated as –4.06 m w.e. (equivalent to –0.41 m w.e. a^{-1}). The difference between cumulative glaciological MB and geodetic MB between 2005 and 2014 is only –0.52 m w.e., which is equivalent to a difference of –0.05 m w.e. a^{-1}. Following Zemp and others (2013, section 3.4), the null hypothesis H_0 (the cumulative glaciological MB is not statistically different from the geodetic MB) is accepted at

https://doi.org/10.3189/2016AoG71A570 Published online by Cambridge University Press

the 95% as well as 90% levels, so the difference between cumulative glaciological MB and geodetic MB between 2005 and 2014 is insignificant. The statistical agreement between the two MBs suggests that the stake and accumulation site network (Section 3) is suitable and able to capture the spatial variability of MB over the glacier, and that no large systematic biases exist in the glaciological method. Consequently, no bias correction was applied to the MB glaciological series.

6. CONCLUSION

A 4 year meteorological dataset (between 1 October 2009 and 30 September 2013), one of the longest high-altitude (4863 m a.s.l.) records in this part of the HKH, was used to describe the meteorology on Chhota Shigri Glacier. A decrease in wind speed and a rapid increase of RH and LWI from the last week of May or the first week of June mark the onset of the monsoon, whereas a sudden drop in RH and LWI and an increase in wind speed around 20 September showed the sharp decay of the monsoon on Chhota Shigri Glacier.

In the main ablation part of the glacier (between 4400 and 5200 m a.s.l.), the mean annual d*b*/d*z* of annual MB, 0.66 m w.e. $(100\,\mathrm{m})^{-1}$, over the 2002–14 period is similar to those observed in the Nepalese Himalaya or on mid-latitude glaciers. The mean annual d*b*/d*z* in the accumulation area (between 5200 and 5500/5550 m a.s.l.) was 0.22 m w.e. $(100\,\mathrm{m})^{-1}$. The glaciological MB series was recalculated assuming a linear area change between 2005 and 2014 and evaluated against the geodetic MB calculated from SPOT5 and Pléiades DEMs. Glaciological and geodetic cumulative MBs are statistically similar (difference of $-0.05\,\mathrm{m\,w.e.\,a^{-1}}$ over 9 years), suggesting that there is no need to apply any bias correction to the glaciological MB. Chhota Shigri Glacier experienced mass wastage between 2002 and 2014 with a cumulative MB of –6.72 m w.e. and a mean B_a of $-0.56 \pm 0.40\,\mathrm{m\,w.e.\,a^{-1}}$. ELA_0 for zero B_a was calculated as ~4950 m a.s.l., corresponding to an AAR_0 of ~61%.

A single year of precipitation data at Chhota Shigri Glacier base camp showed that this glacier received maximum accumulation during the winter months. In addition, the comparison of 4 years of seasonal mass balances (B_w and B_s) with meteorological variables suggested that there is a co-occurrence of ablation and accumulation during the summer months and that the intensity of summer accumulation (i.e. monsoon) controls the B_a evolution through controlling the B_s. However the present analysis, conducted over 4 years only, needs to be confirmed by longer-term studies of glaciological seasonal MBs and meteorological variables. The B_a series of Chhota Shigri Glacier since 2002 is the longest continuous B_a series in the HKH region and should be continued to use this glacier as a benchmark for climate change studies.

ACKNOWLEDGEMENTS

This work has been supported by IFCPAR/CEFIPRA project No. 3900-W1, the French Service d'Observation GLACIOCLIM, a grant from Labex OSUG@2020 (Investissements d'avenir – ANR10 LABX56) as well as support from CHARIS, INDICE, SAC and Department of Science and Technology (DST), Government of India. M.F. Azam is grateful to IRD for providing financial support for his PhD. A special thanks to our field assistant Adhikari Ji and the porters who have taken part in successive field trips, sometimes in harsh conditions. We thank Jawaharlal Nehru University for providing the facilities to carry out this work. E.B. acknowledges support from the French Space Agency (CNES) through the TOSCA and ISIS program. We are also grateful to two anonymous referees and the Chief Editor Graham Cogley, whose thorough comments significantly improved the paper.

REFERENCES

Ageta Y and Higuchi K (1984) Estimation of mass balance components of a summer-accumulation type glacier in the Nepal Himalaya. *Geogr. Ann. A*, **66**, 249–255

Azam MF and 10 others (2012) From balance to imbalance: a shift in the dynamic behaviour of Chhota Shigri Glacier (western Himalaya, India). *J. Glaciol.,* **58,** 315–324 (doi: 10.3189/2012JoG11J123)

Azam MF, Wagnon P, Vincent C, Ramanathan AL, Linda A and Singh VB (2014a) Reconstruction of the annual mass balance of Chhota Shigri Glacier (western Himalaya, India) since 1969. *Ann. Glaciol.*, **55**(66), 69–80 (doi: 10.3189/2014AoG66A104)

Azam MF and 6 others (2014b) Processes governing the mass balance of Chhota Shigri Glacier (western Himalaya, India) assessed by point-scale surface energy balance measurements. *Cryosphere*, **8**, 2195–2217 (doi: 10.5194/tc-8-2195-2014)

Berthier E and 10 others (2014) Glacier topography and elevation changes derived from Pléiades sub-meter stereo images. *Cryosphere*, **8**, 2275–2291 (doi: 10.5194/tc-8-2275-2014)

Bhutiyani MR, Kale VS and Pawar NJ (2010) Climate change and the precipitation variations in the northwestern Himalaya: 1866–2006. *Int. J. Climatol.*, **30**(4), 535–548

Bolch T and 11 others (2012) The state and fate of Himalayan glaciers, *Science,* **336**, 310–314

Brun F and 8 others (2015) Seasonal changes in surface albedo of Himalayan glaciers from MODIS data and links with the annual mass balance. *Cryosphere,* **9**, 341–355 (doi: 10.5194/tc-9-341-2015)

Cogley JG (2009) Geodetic and direct mass-balance measurements: comparison and joint analysis. *Ann. Glaciol.,* **50,** 96–100

Cuffey KM and Paterson WSB (2010) *The physics of glaciers*, 4th edn. Butterworth-Heinemann, Oxford

Datt P, Srivastava PK, Negi PS and Satyawali PK (2008) Surface energy balance of seasonal snow cover for snow-melt estimation in N-W Himalaya. *J. Earth Syst. Sci.*, **117**, 567–73

Dimri AP and Dash SK (2012) Wintertime climatic trends in the western Himalayas. *Climatic Change*, **111**(3–4), 775–800

Dimri AP and Mohanty UC (2009) Simulation of mesoscale features associated with intense western disturbances over western Himalayas. *Meteorol. Appl.,* **16**, 289–308

Fowler HJ and Archer DR (2006) Conflicting signals of climatic change in the Upper Indus Basin. *J. Climate*, **19**, 4276–4293

Fujita K (2008) Effect of precipitation seasonality on climatic sensitivity of glacier mass balance. *Earth Planet. Sci. Lett.*, **276**(1), 14–19

Fujita K and Nuimura T (2011) Spatially heterogeneous wastage of Himalayan glaciers. *Proc. Natl Acad. Sci., USA (PNAS)*, **108**, 14 011–14 014 (doi: 10.1073/pnas.1106242108)

Gardelle J, Berthier E, Arnaud Y and Kääb A (2013) Region wide glacier mass balances over the Pamir Karakoram Himalaya during 1999–2011. *Cryosphere*, **7**, 1263–1286 (doi: 10.5194/tc-7-1263-2013)

Huss M (2013) Density assumptions for converting geodetic glacier volume change to mass change. *Cryosphere*, **7**, 877–887 (doi: 10.5194/tc-7-877-2013)

Immerzeel WW, Van Beek LPH and Bierkens MFP (2010) Climate change will affect the Asian water towers. *Science*, **328**, 1382–1385

https://doi.org/10.3189/2016AoG71A570 Published online by Cambridge University Press

Kääb A, Berthier E, Nuth C, Gardelle J and Arnaud Y (2012) Contrasting patterns of early 21st century glacier mass change in the Himalaya. *Nature,* **488**(7412), 495–498 (10.1038/nature11324)

Kääb A, Treichler D, Nuth C and Berthier E (2015) Brief Communication: Contending estimates of 2003–2008 glacier mass balance over the Pamir–Karakoram–Himalaya. *Cryosphere*, **9**, 557–564 (doi: 10.5194/tc-9-557-2015)

Kaser G, Großhauser M and Marzeion B (2010) Contribution potential of glaciers to water availability in different climate regimes. *Proc. Natl Acad. Sci. USA (PNAS)*, **107**, 20 223–20 227 (doi: 10.1073/pnas.1008162107)

Lang TJ and Barros AP (2004) Winter storms in central Himalayas. *J. Meteorol. Soc. Jpn*, **82**(3), 829–844

Mölg T, Maussion F, Yang W and Scherer D (2012) The footprint of Asian monsoon dynamics in the mass and energy balance of a Tibetan glacier. *Cryosphere*, **6**, 1445–1461 (doi: 10.5194/tc-6-1445-2012)

Paterson WSB (1994) *The physics of glaciers*, 3rd edn. Elsevier, Oxford

Paul F, Kääb A and Haeberli W (2007) Recent glacier changes in the Alps observed by satellite: consequences for future monitoring strategies. *Global Planet. Change*, **56**, 111–122

Prasad VH and Roy P (2005) Estimation of snowmelt runoff in Beas Basin, India. *Geocarto Int.*, **20**(2), 41–47

Rabatel A, Dedieu JP and Vincent C (2005) Using remote-sensing data to determine equilibrium-line altitude and mass-balance time series: validation on three French glaciers, 1994–2002. *J. Glaciol.*, **51**, 539–546 (doi: 10.3189/172756505781829106)

Racoviteanu A, Armstrong R and Williams M (2013) Evaluation of an ice ablation model to estimate the contribution of melting glacier ice to annual discharge in the Nepal Himalaya. *Water Resour. Res.*, **49**, 5117–5133

Shea JM, Menounos B, Moore RD and Tennant C (2013) An approach to derive regional snow lines and glacier mass change from MODIS imagery, western North America. *Cryosphere*, **7**, 667–680 (doi: 10.5194/tc-7-667-2013)

Shea JM, Wagnon P, Immerzeel WW, Biron R and Brun F (2015) A comparative high-altitude meteorological analysis from three catchments in the Nepal Himalaya. *Int. J. Water Res. Dev.*, **31**(2), 174–200 (doi: 10.1080/07900627.2015.1020417)

Shekhar M, Chand H, Kumar S, Srinivasan K and Ganju A (2010) Climate-change studies in the western Himalaya. *Ann. Glaciol.*, **51**, 105–112 (doi: 10.3189/172756410791386508)

Sicart JE, Hock R, Ribstein P, Litt M and Ramirez E (2011) Analysis of seasonal variations in mass balance and meltwater discharge of the tropical Zongo Glacier by application of a distributed energy balance model. *J. Geophys. Res.*, **116**, D13105 (doi: 10.1029/2010JD015105)

Thayyen RJ and Gergan JT (2010) Role of glaciers in watershed hydrology: a preliminary study of a 'Himalayan catchment'. *Cryosphere,* **4,** 115–128

Thibert E, Blanc R, Vincent C and Eckert N (2008) Glaciological and volumetric mass-balance measurements: error analysis over 51 years for Glacier de Sarennes, French Alps. *J. Glaciol.,* **54**(186), 522–532 (doi: 10.3189/002214308785837093)

Vincent C and 10 others (2013). Balanced conditions or slight mass gain of glaciers in the Lahaul and Spiti region (northern India, Himalaya) during the nineties preceded recent mass loss. *Cryosphere,* **7,** 569–582 (doi: 10.5194/tc-7-569-2013)

Wagnon P and 10 others (2007) Four years of mass balance on Chhota Shigri Glacier, Himachal Pradesh, India, a new benchmark glacier in the western Himalaya. *J. Glaciol.,* **53,** 603–611

Wagnon P and 11 others (2013) Seasonal and annual mass balances of Mera and Pokalde glaciers (Nepal Himalaya) since 2007. *Cryosphere*, **7**, 1769–1786 (doi: 10.5194/tc-7-1769-2013)

Zemp M, Hoelzle M and Haeberli W (2009) Six decades of glacier mass-balance observations: a review of worldwide monitoring network. *Ann. Glaciol.*, **50**(50), 101–111

Zemp M and 16 others (2013) Reanalysing glacier mass balance measurement series. *Cryosphere*, **7**, 1227–1245 (doi: 10.5194/tc-7-1227-2013)

Zhang G and 10 others (2013) Energy and mass balance of the Zhadang Glacier surface, central Tibetan Plateau. *J. Glaciol.*, **213**, 137–148 (doi: 10.3189/2013JoG12J152)

https://doi.org/10.3189/2016AoG71A570 Published online by Cambridge University Press